

DIURNAL VARIATIONS IN BOUNDARY LAYER WINDS OVER THE SOUTH-CENTRAL UNITED STATES IN SUMMER

WILLIAM D. BONNER¹ and JAN PAEGLE²

Department of Meteorology, University of California, Los Angeles, Calif.

ABSTRACT

Analysis of 1 week's data in August 1960 shows significant diurnal variations in surface geostrophic wind over the south-central United States. The oscillation in the southerly component (V_g) is driven by the response of the thermal wind to the diurnal temperature cycle over sloping terrain. A smaller oscillation in U_g derives from spatial variations in the amplitude of the diurnal pressure wave. The amplitude of the oscillation in V_g is about 3 to 5 m sec⁻¹ at the surface, decaying exponentially with height to near 0 at 2 km.

Examination of 11 yr of summertime rawinsonde data at Fort Worth, Tex., shows a very regular diurnal variation in boundary layer wind with maximum amplitude of about 3 m sec⁻¹ at 600 m above the ground. This oscillation is forced by periodic variations in both eddy viscosity and geostrophic wind. Using a simplified model of the boundary layer, we obtain solutions for the diurnally periodic wind resulting from "reasonable" variations in eddy viscosity and "observed" variations in geostrophic wind.

1. INTRODUCTION

Boundary layer winds oscillate diurnally reaching a maximum speed at night and a minimum during the day at elevations between about 30 and 2000 m above the ground. The amplitude of this oscillation is 2 to 3 m sec⁻¹ at levels between 0.5 and 1.0 km above the ground (Hering and Borden 1962). Maximum speed occurs between 00 and 03 local time (LT) (Bonner 1968).

The wind variation is especially pronounced with southerly flow along the central plains to the east of the Rocky Mountains. In this region, superposition of a strong diurnal oscillation upon the large-scale geostrophic flow may lead to nocturnal jet streams with speeds of more than 25 m sec⁻¹ within the first kilometer above the ground (Bonner et al. 1968).

Boundary layer wind oscillations may arise from periodic variations in the horizontal pressure force as in mountain valley wind circulations, or they may be driven by day-to-night variations in the frictional stress. Numerical experiments with constant geostrophic wind and diurnally varying eddy viscosity duplicate reasonably well the observed oscillations over the central plains (Buajitti and Blackadar 1957, Estoque 1963, and Krishna 1968). While this mechanism alone may explain the oscillation over level terrain, it has become increasingly apparent that there is a strong diurnal variation in the surface geostrophic wind just east of the Rocky Mountains (Hoecker 1965 and Sangster 1967).

Using the altimeter correction system of Bellamy (1945), Sangster (1967) has shown a day-to-night change in geostrophic wind as large as 9 m sec⁻¹ in northern Texas. Minimum speed occurs near 06 CST, maximum speed near 16 CST. An oscillation this large and nearly 180° out of

phase with the oscillation of the real wind certainly cannot be ignored in explanations of the low-level jet.

As a corroboration and extension of Sangster's work, we have attempted to describe the diurnal variation of geostrophic wind over the Great Plains, its variation with altitude, and its interaction with the viscous forcing function to produce the observed variation in boundary layer wind. Sections 2 and 3 describe variations in low-level geostrophic winds in Texas and Oklahoma during a 1-week period in August 1960. Section 4 describes observed variations in boundary layer wind as determined from two sets of data that are combined to give the equivalent of 3-hr observations of the wind. In section 5, we examine the effects of variable viscosity and variable pressure-gradient force upon the boundary layer wind, comparing derived results with observations in section 4.

2. VARIATIONS IN SURFACE GEOSTROPHIC WIND

Using the altimeter correction system of Bellamy (1945), one may write the eastward and northward components of the surface geostrophic wind as

$$U_g = -\frac{g}{f}(1+S^*)\frac{\partial D}{\partial y} + S^*\frac{g}{f}\frac{\partial z}{\partial y} \quad (1)$$

and

$$V_g = \frac{g}{f}(1+S^*)\frac{\partial D}{\partial x} - S^*\frac{g}{f}\frac{\partial z}{\partial x}$$

where z is the height of the terrain, S^* is the specific virtual temperature anomaly

$$S^* = \frac{T^* - T_p}{T_p} \quad (2)$$

and D is the difference $z - zp$ at terrain height. Variables T_p and z_p are temperature and pressure altitude in the standard atmosphere. Thus, each component of the surface geostrophic wind is a sum of two terms, one depending

¹ Now at the Techniques Development Laboratory, Weather Bureau, ESSA, Silver Spring, Md.

² Now at the University of Utah at Salt Lake City

primarily upon the gradient of D values along the sloping terrain, the other upon the product of specific temperature anomaly S^* and the terrain slope.

Suppose, for simplicity, that the gradient of terrain is in the minus x direction and that the average daily value of S^* is zero. In the morning, a negative S^* gives a negative contribution to V_g . If there is no counterbalancing oscillation in $\partial D/\partial x$, there will be a diurnal oscillation of the geostrophic wind with an amplitude that depends upon the terrain slope and the amplitude of the diurnal temperature wave. In the case of southerly flow east of the Rocky Mountains, the geostrophic wind will oscillate in phase with the temperature cycle—reaching maximum speed at the time of maximum temperature. With northerly winds or with a reversal in terrain slope, the sense of the oscillation is reversed with maximum speed at the time of minimum temperature.

METHOD

Geostrophic surface winds were computed from equations (1) at 28 grid points in Texas and Oklahoma (fig. 1). Grid points are at intervals of 1° latitude and 1.25° longitude. Centered differences were used so that the basic length unit is approximately 220 km.

Use of equations (1) requires a smoothed representation of the terrain. We used a determination by McClain (1960) of average terrain heights within areas bounded by 1° latitude and longitude lines (fig. 2). Terrain heights were interpolated at grid points; values of $\partial z/\partial x$ and $\partial z/\partial y$ were computed from centered finite differences and then smoothed to represent only the large-scale features of terrain.

Altimeter settings, temperatures, and dew points were tabulated at 3-hr intervals at approximately 50 stations in the area of interest. Altimeter settings were converted to D values (see, for example, Haltiner and Martin 1957), temperatures and dew points to virtual temperature T^* . Virtual temperatures and D values were averaged over the period from Aug. 2 to 8, 1960, and maps were constructed of mean D and T^* fields at 00, 03, 06, . . . , 21 cstr. Virtual temperatures were converted to specific temperature anomalies (equation 2), and values of S^* , D , $\partial z/\partial x$, $\partial z/\partial y$ at grid points were used to compute U and V components of the surface geostrophic wind.

RESULTS

Figure 3 shows isotachs of the mean geostrophic wind at 00, 06, 12, and 18 cstr for the period from Aug. 2 to 8, 1960. Geostrophic winds during the period were constantly from the south or southwest. Fronts remained to the north of the area, and skies were mainly clear except for afternoon showers and thunderstorms in Texas and scattered nocturnal thunderstorms in Oklahoma.

Each map shows a zone of strong geostrophic wind between 96° and 98° W. There is a weak maximum in Oklahoma and a second stronger maximum in central Texas. Strongest computed winds are 13.7 m sec^{-1} at 06 cstr and 23.7 m sec^{-1} at 18 cstr.

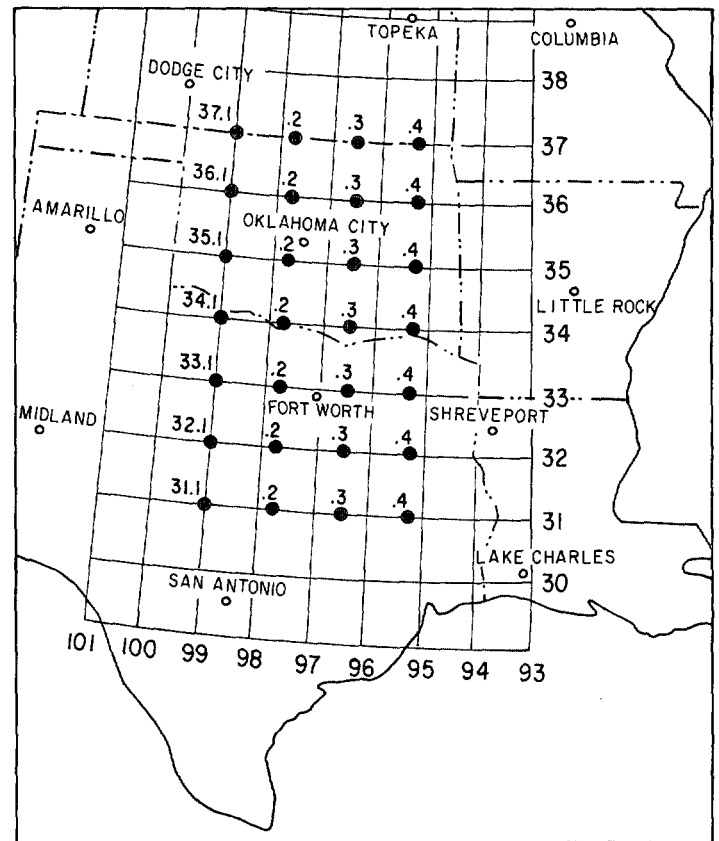


FIGURE 1.—Grid used in determination of geostrophic winds. Grid point separation is 1° latitude by 1.25° longitude. The map shows the position of radiosonde stations used in thermal wind calculations (section 3).

Sangster (1967) determined the average geostrophic south wind component between Amarillo and Oklahoma City for the month of June 1966 to be 6 m sec^{-1} at 06 cstr and 15 m sec^{-1} at 18 cstr. Our values in this area for the shorter period in August 1960 are 7 m sec^{-1} and 15 m sec^{-1} , respectively.

Figure 4 shows the time variation in the northward V component of the geostrophic wind at two locations in Oklahoma. Near Oklahoma City (grid point 35.2 in fig. 1), the oscillation is quite regular with minimum V_g near 0430 cstr and a maximum near 17 cstr. At grid point 36.4 in northeastern Oklahoma, the terrain slopes upward to the east (fig. 2). Here, the sense of the oscillation is changed with minimum geostrophic speed during the afternoon and maximum speed near 06 cstr.

Daily variations in U_g and V_g are summarized in figures 5, 6, and 7 that represent averages of the geostrophic components at 12 grid points in figure 1.

Total U_g and V_g components are shown in figure 5. On the average, minimum V_g occurs between 03 and 06 cstr and maximum V_g near 17 cstr. The total variation in southerly geostrophic wind from morning to evening is about 7.5 m sec^{-1} . Changes are roughly in phase with the diurnal temperature wave; however, largest V_g occurs about 2 hr after the time of maximum temperature. The U_g component is strongest near noon, weakest near 21 cstr, and undergoes a total variation of about 2.5 m sec^{-1} .

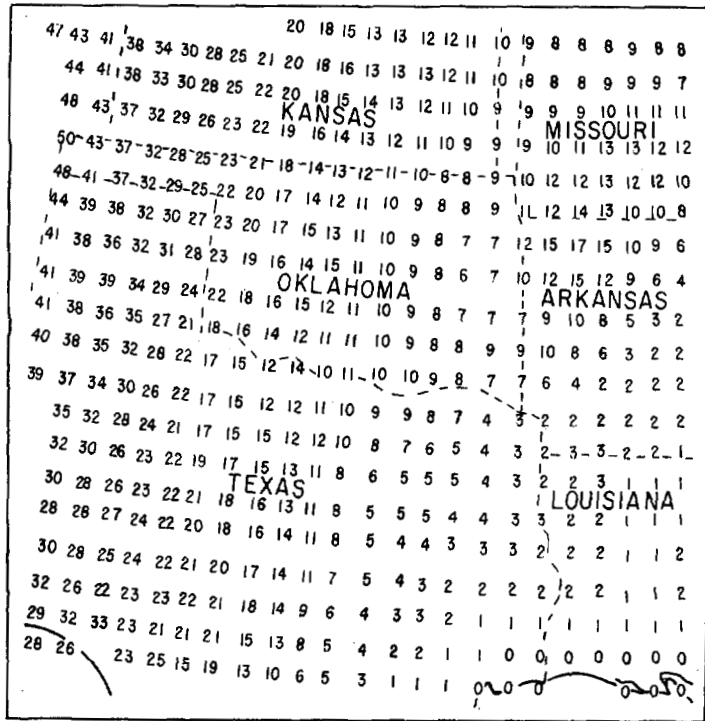


FIGURE 2.—Terrain heights in hundreds of feet within areas bounded by 1° latitude and longitude lines, taken from data used by McClain (1960) in construction of a smoothed topographic map.

Diurnal variations in the contribution to U_g and V_g from the terrain slope term (fig. 6) are roughly as expected with minimum and maximum values at 06 and 15 CST. Total variations in U_g and V_g from the second terms in equations (1) are 0.8 and 5.4 m sec⁻¹, respectively.

The upper half of figure 7 shows that the observed variations in U_g result primarily from a diurnal variation in the y derivative of D values at the level of the terrain. This effect dominates the terrain slope term at most locations enhancing the westerly geostrophic winds in the late morning and early afternoon. The V_g component in the lower half of figure 7 shows a relatively small, primarily semidiurnal oscillation with a maximum contribution near 18 CST, a relative maximum near 06 CST, and minima near 03 and 10 CST.

3. VARIATIONS IN THERMAL WIND

By subtracting the component equations at two levels a constant height above the ground and using the hydrostatic relationship $\partial D/\partial z = S^*/(1+S^*)$, the following expressions are derived for the thermal wind:

$$U_{th} = -g \frac{\Delta z}{f} \frac{\partial}{\partial y} \overline{\left(\frac{S^*}{1+S^*} \right)} + \frac{g}{f} (S_1^* - S_0^*) \frac{\partial z}{\partial y}$$

and

$$V_{th} = g \frac{\Delta z}{f} \frac{\partial}{\partial x} \overline{\left(\frac{S^*}{1+S^*} \right)} - \frac{g}{f} (S_1^* - S_0^*) \frac{\partial z}{\partial x}$$

The bar indicates an average value in the layer from 0 to 1 of thickness Δz . Equations (3) neglect small terms

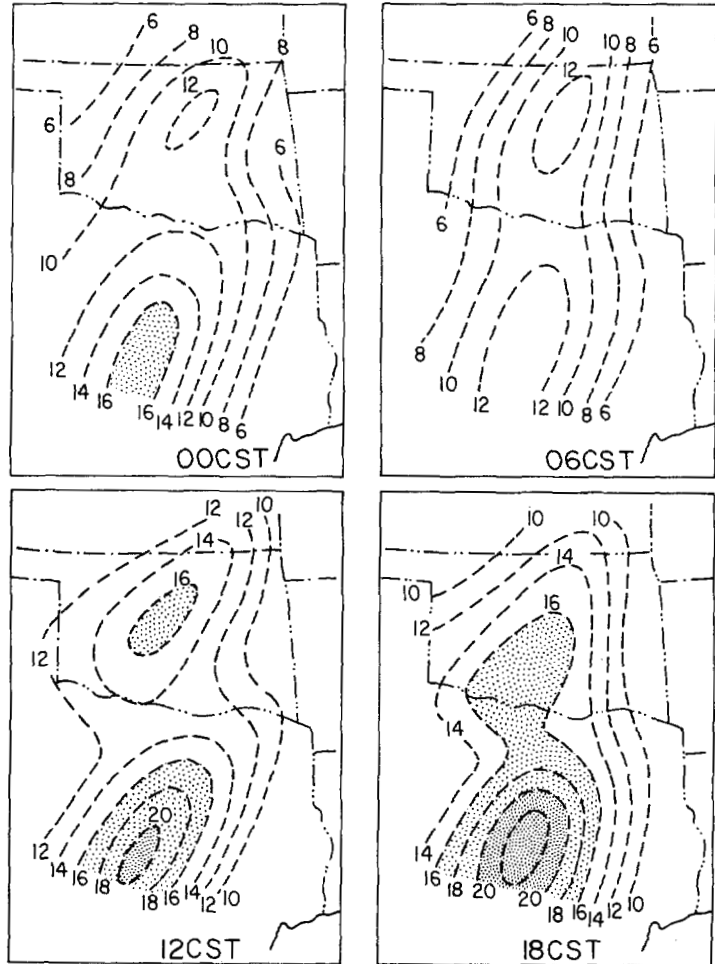


FIGURE 3.—Isotachs (meters per second) of average geostrophic wind from Aug. 2 to 8, 1960.

arising from the S^* factor in the first terms of equations (1).

The first terms in equations (3) represent primarily the gradient of S^* in layers parallel to the terrain. The second term depends upon the vertical variation of S^* and the terrain slope.

METHOD AND ILLUSTRATION

As an example, figure 8 shows the T^* and S^* curves from mean data for Fort Worth, Tex., at 06 and 18 CST. During the afternoon, S^* decreases with height. Since $\partial z/\partial x$ is negative, the second term in the expression for V_{th} (equations 3) is negative and acts to decrease the strong southerly geostrophic wind at the surface. At 06 CST, S^* is constant or increasing with height and the second term is small or acting in the opposite sense.

Similar curves were constructed from the average temperature data from each of 11 radiosonde stations in figure 1. Mean values of $S^*/(1+S^*)$ in 400-m layers were determined for each station at each time. These values were plotted and analyzed, and first terms were computed from values interpolated at grid points. Sample analyses of $S^*/(1+S^*)$ are shown in figure 9. At both 06 and 18 CST,

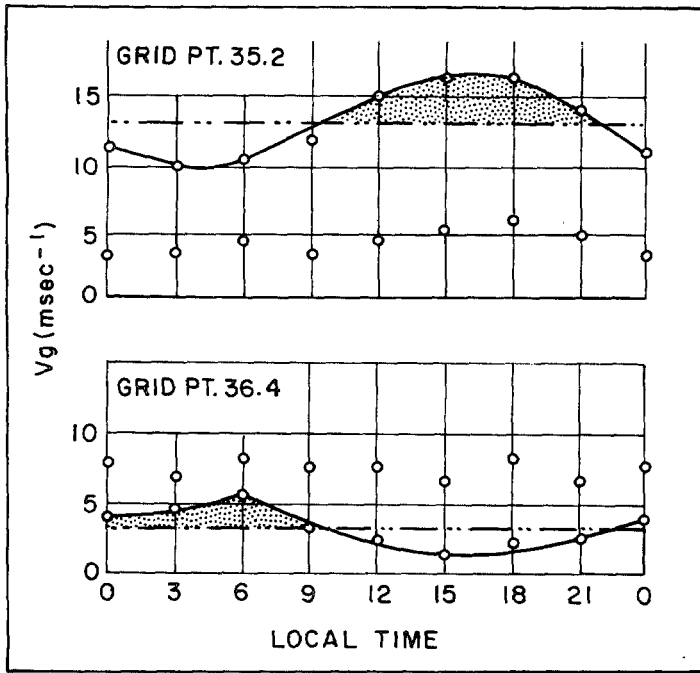


FIGURE 4.—Southerly component of geostrophic wind at grid points 35.2 and 36.4 (see also fig. 1). The values are averages from Aug. 2 to 8, 1960. Smooth curves connect points representing total geostrophic wind. Unconnected points are contributions from the D value term alone. Note the phase reversal with the reversal of terrain slope.

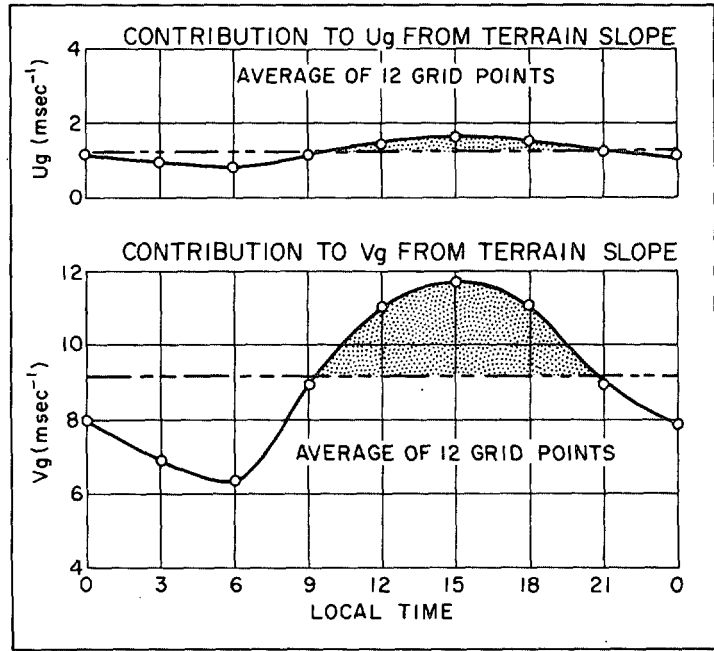


FIGURE 6.—Time variation of terrain contribution to geostrophic wind, averaged over the same grid points as in figure 5.

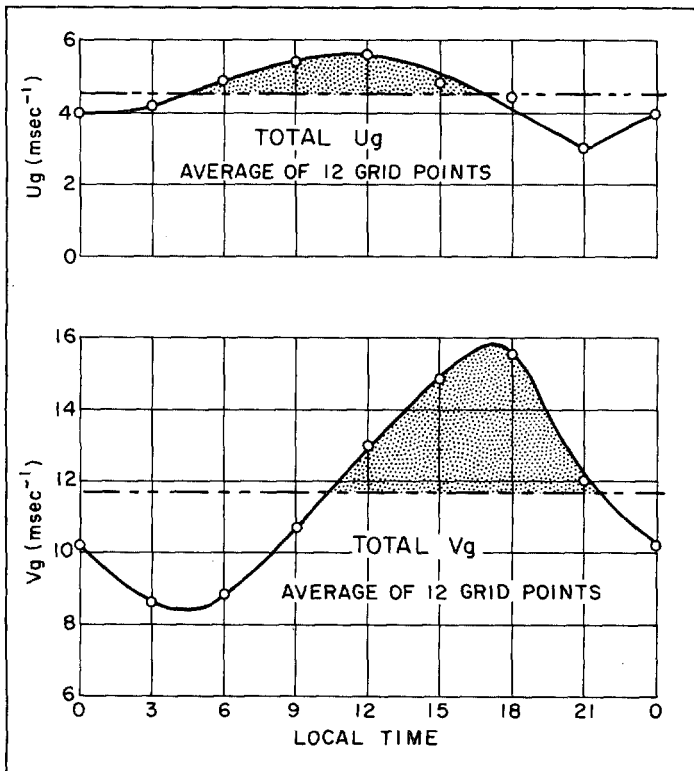


FIGURE 5.—Time variation of total geostrophic wind, average of 12 grid points in western Oklahoma and north-central Texas.

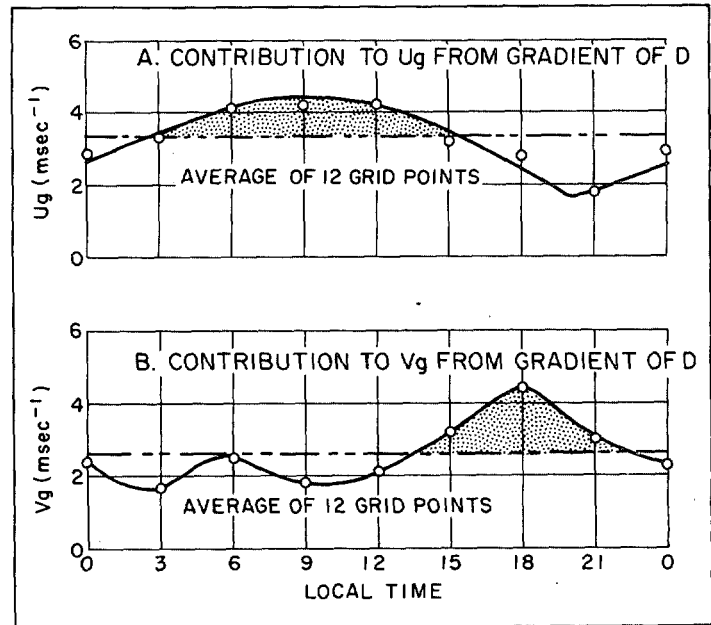


FIGURE 7.—Time variation of the contribution to geostrophic wind from the gradient of D values, averaged over the same grid points as in figure 5.

warmest air lies over the northwestern section of the region. Thermal winds from this term parallel the isopleths of $S^*/(1+S^*)$ and shift from northeasterly during the morning to northerly during the afternoon—acting at the later time to diminish with height the strong southerly surface geostrophic winds.

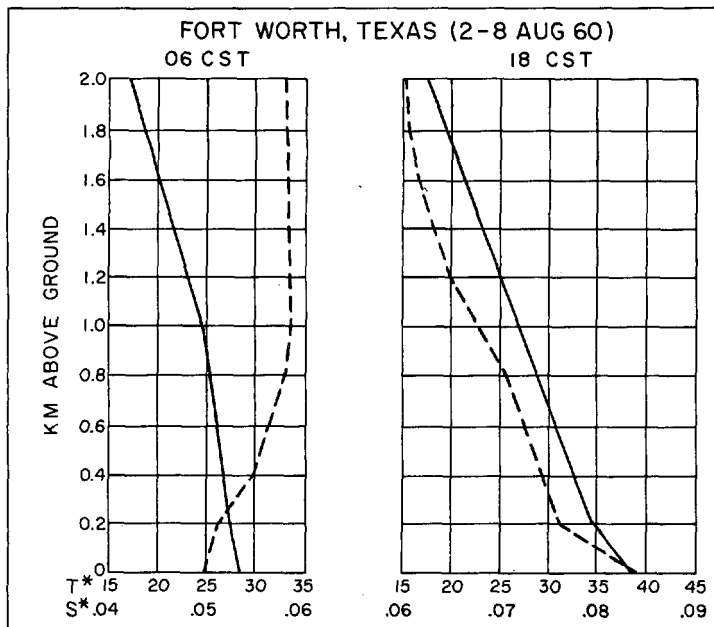


FIGURE 8.—Height and time variation of T^* (solid lines) and S^* (dashed lines) at Fort Worth, Tex., averaged over the week from Aug. 2 to 8, 1960.

RESULTS

Figure 10 shows thermal winds computed from equations (3) at 06 and 18 csr and the vector change in thermal wind between the two observation times. At 06 csr, thermal winds within the first 2 km are directed mainly from the east-northeast with speeds of roughly 4 to 7 m sec⁻¹. At 18 csr, thermal winds are from the north-northeast with speeds of 8 to 12 m sec⁻¹ through most of the region. Changes in thermal wind are parallel to the terrain contours and are northerly where the terrain slopes down to the east and southerly where the terrain slope reverses (grid points 37.4 and 36.4). Vector changes in figure 10 show a variation in thermal wind within the first 2 km that is nearly equal and opposite to the variation in surface geostrophic wind. Addition of the V components of the thermal winds in figure 10 to the 06 and 18 csr surface winds in figure 3 yields geostrophic southerly winds at 2 km that are essentially the same at 06 and 18 csr. Since 06 and 18 csr are near the times of minimum and maximum surface geostrophic wind, the amplitude of the implied surface oscillation is roughly one-half the magnitude of the thermal wind changes in figure 10.

The oscillation in thermal wind is shown schematically in figure 11. Physically, the process is quite simply and roughly as Sangster describes. At 2 km, the geostrophic wind does not vary from day to night. At night, air above the higher terrain cools much more than the air at the same pressure level farther to the east. This introduces a southerly component to the thermal wind that implies that V_g at the surface is less than V_g at 2 km. During the

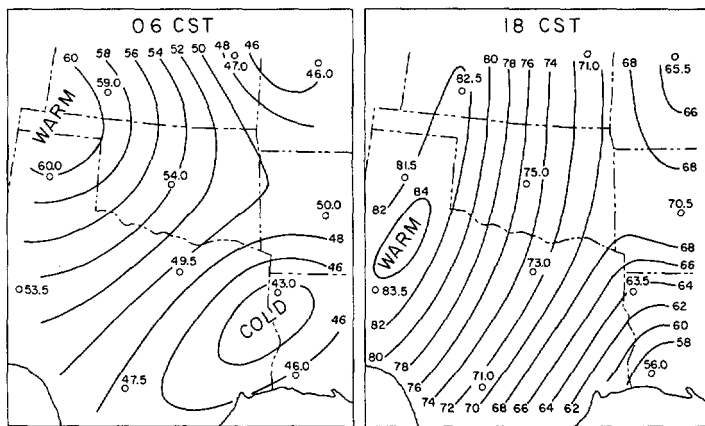


FIGURE 9.—Fields of $S^*/(1+S^*)$ from the surface to 400 m above the ground. Values have been multiplied by 10^3 . Note the warm tongue to the west and the change in orientation and spacing of the lines between 06 and 18 csr.

the day, the air over the mountains becomes warmer than the air to the east; V_{th} is from the north, and V_g at the surface becomes larger than V_g at 2 km. Thus, the oscillation in the surface geostrophic wind is driven by an alternating thermal wind that results from the daily heating cycle over sloping terrain. The picture is a simplification of the thermal wind patterns in figure 10 where a mean temperature gradient from east to west keeps a northerly component to the thermal winds at both 06 and 18 csr. However, the important feature is the pronounced daytime increase in the northerly component of the thermal wind (fig. 10) that produces an afternoon maximum in the southerly component of the surface geostrophic wind.

Figure 12 shows the rate of decay of this oscillation with height as determined from thermal wind calculation in 400-m layers. The graph is based upon changes in the V component of the geostrophic wind at 15 grid points and assumes that there is no significant shift in the phase of the oscillation with height. At each level, the change in V_g was expressed as a percentage of the surface change. Percentages at individual grid points were then averaged to obtain the plotted points in figure 12. The decay with height is logarithmic and follows very closely the relationship $r = e^{-z/0.8}$ where z is in kilometers above the ground and r is the ratio between the amplitude at z and the surface amplitude.

4. VARIATIONS IN OBSERVED WIND

The period Aug. 2 to 8, 1960, was chosen initially because of a high frequency of morning low-level jet observations (Bonner 1968), and winds during this period do show strong and regular diurnal variations. Our aim, however, is not to describe the particular events from August 2 to 8, but to provide a much more general description of the diurnal oscillation in boundary layer wind.

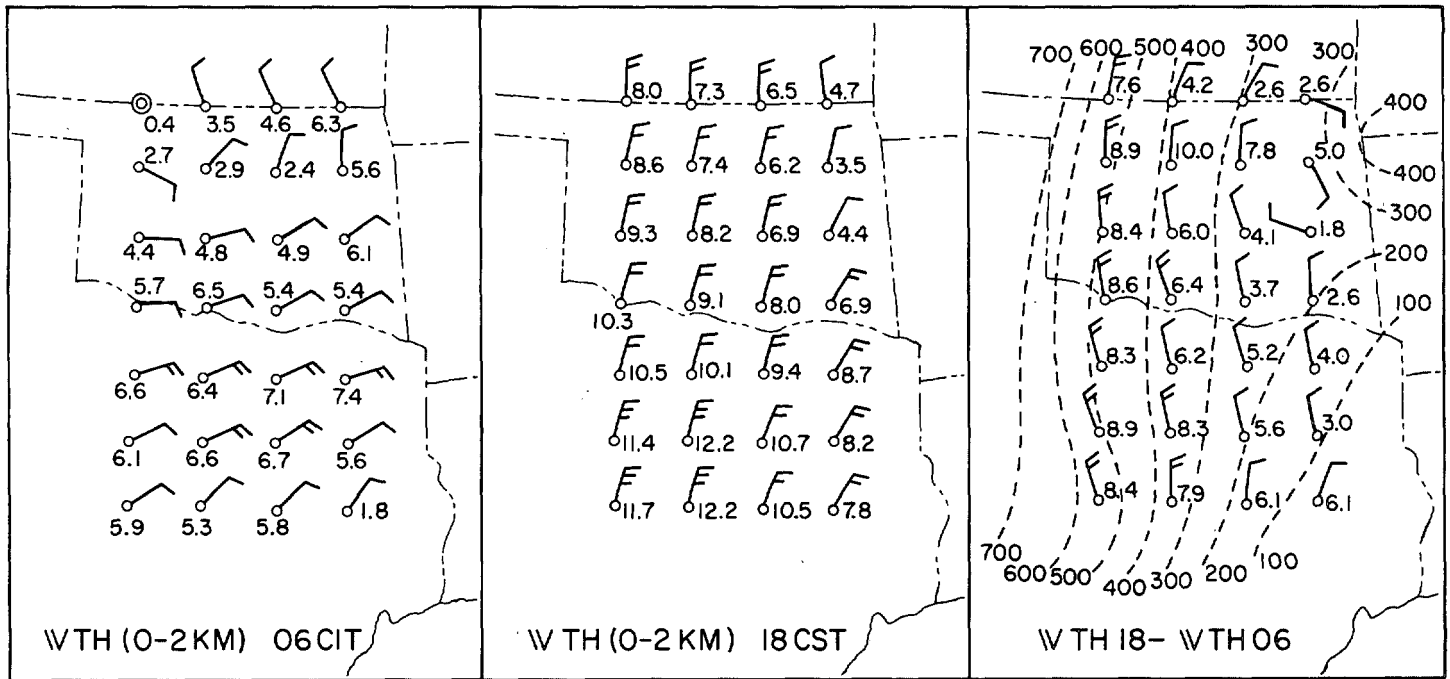


FIGURE 10.—Thermal winds from the surface to 2 km and the change in thermal wind from 06 to 18 cst. Values at grid points are in meters per second. Winds are plotted in standard synoptic form with barbs representing speeds in knots. Dashed lines are mean terrain contours from figure 2 labeled in meters above sea level.

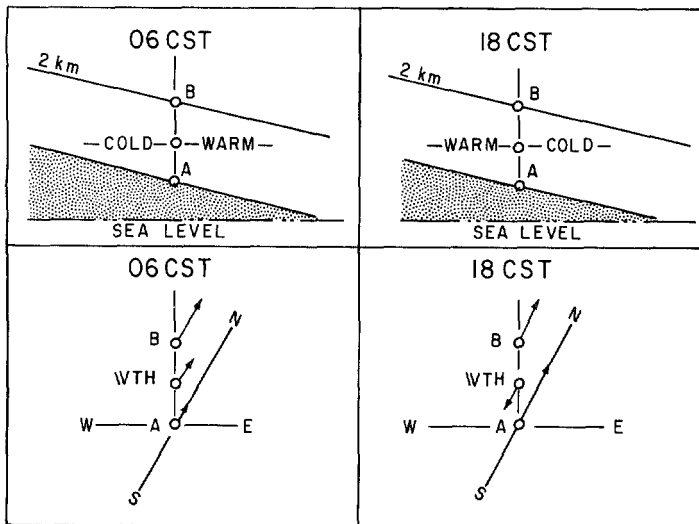


FIGURE 11.—Schematic representation of oscillation in thermal wind.

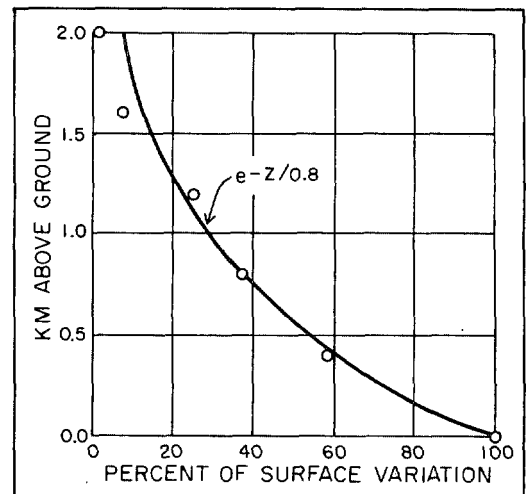


FIGURE 12.—Decay of the oscillation with height. The values follow closely a curve with equation $r = e^{-z/0.8}$ where z is in kilometers above the ground and r is the percentage of the surface oscillation at level z .

For this purpose, we examined daily rawinsonde observations at Fort Worth, Tex., for July and August 1952 to 1955 and 1958 to 1964. During the earlier period, observations were regularly scheduled at 03, 09, 15, and 21 GMT; for the later period, observation times were 00, 06, 12, and 18 GMT. By combining the two series of observations, it is possible to obtain the equivalent of 3-hr observations of the wind. The same technique has been used by Harris et al. (1966), Harris (1959), and Johnson (1955) to obtain first and second harmonics of daily variations in wind,

pressure, and temperature. Levels examined that are common to both series include the surface, 0.5, 1.0, 2.0, 2.5, and 3.0 km above sea level.

At each observation time, we computed the deviation of the wind from its average value for the particular day. Deviations were averaged over all days in each series, and the two series were combined to give the average variation shown in figure 13.

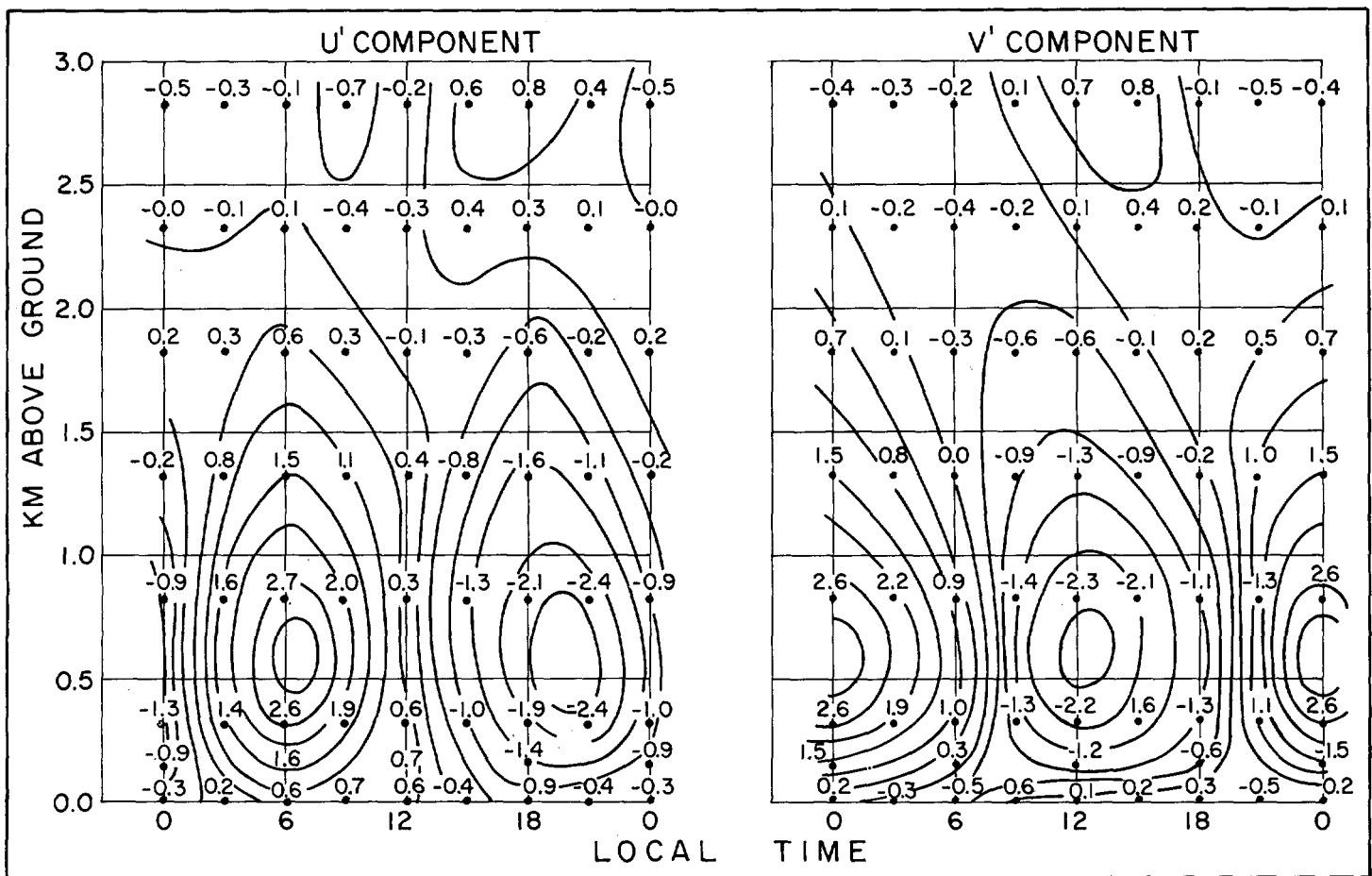


FIGURE 13.—Time variation of the deviations in wind from its daily mean value at Fort Worth, Tex. Values are in meters per second. Observations at 00, 06, etc., are averages for July and August 1958–1964. Observations at 03, 09, etc., are averages for July and August 1952–1955.

Both components of the wind show a daily variation of 5 to 6 m sec⁻¹ between about 400 and 800 m above the ground. Maximum westerly wind occurs between 06 and 07 csl; maximum southerly wind near 00 csl. The level of maximum amplitude in both components is approximately 600 m above the ground, and the oscillation disappears between 2.0 and 2.5 km above the ground.

Figure 14 shows hodographs of the wind variations at selected levels above the ground. At 0.15 km, observations exist only for the later period. At the surface, observations could not be combined, but both sets of data indicate counterclockwise rotation of the deviation vector with time. At other levels, rotation is clockwise at a rate that appears to be greatest at night, slowest during the afternoon. Hodographs are nearly circular, with slightly reduced amplitude during the afternoon.

The size of the data circles in figure 14 indicates the probable error in the estimate of each mean deviation vector as determined from the relationship $r=0.939 \bar{d}/\sqrt{n}$ (Chapman 1951) where r is the radius of the probable error circle, \bar{d} is the mean distance between the vector end point for each individual year and the n -yr mean. Hodographs are, in general, well determined, with r approxi-

mately an order of magnitude smaller than the deviation vector itself. The tendency for larger probable errors at 03, 09, etc. is a reflection of the smaller number of years in the earlier data sample.

5. THEORETICAL SOLUTIONS FOR THE BOUNDARY LAYER WIND

In this section, we use a model developed by Paegle (1970) to examine the effects of diurnally periodic eddy viscosity and pressure gradient force on the boundary layer wind. Specifically, we consider (1) time dependent eddy viscosity, constant geostrophic wind; (2) constant eddy viscosity, variable geostrophic wind; and (3) variable viscosity, variable geostrophic wind.

The first problem has been treated by Buajitti and Blackadar (1957), Ooyama (1957), Estoque (1963), and Krishna (1968); the second by Lettau (1964) and Holton (1967); and the third by Sangster (1970) and Paegle (1970).

METHOD

Here, we will briefly outline the model and the method

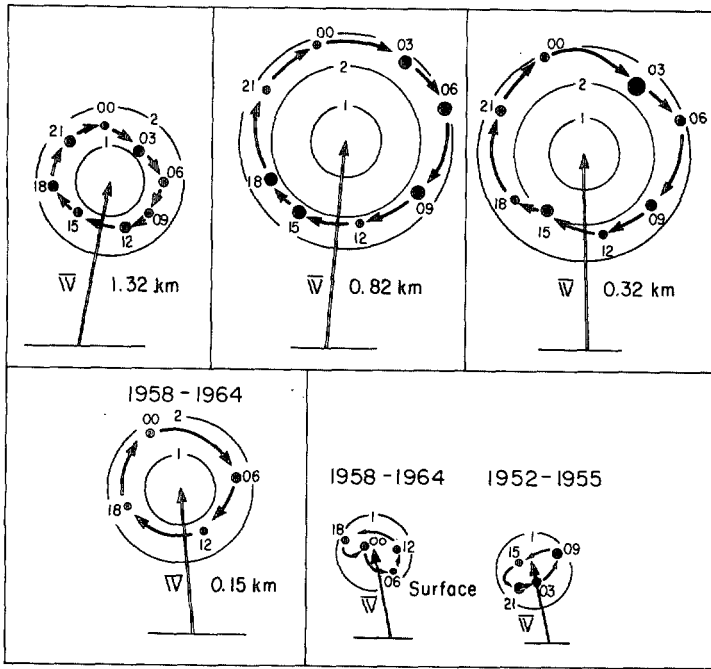


FIGURE 14.—Hodographs of the wind variations at selected levels (same data as in fig. 13). Size of the data circle indicates probable errors in determination of the mean deviation vector. Heights are in meters above the ground; times are CST.

of solution. A more complete description is given by Paegle (1970).

In the complex plane, the horizontal momentum equation may be written

$$\frac{\partial}{\partial t'} (U + iV) + if(U + iV) = if(U_g + iV_g) + K \frac{\partial^2 (U + iV)}{\partial z^2} \quad (4)$$

where (U_g, V_g) are eastward and northward components of the geostrophic wind, t' is time, and K is the eddy viscosity. The geostrophic wind can have an arbitrary time and height dependence; the eddy viscosity may be time dependent, but is assumed to be constant in height. Non-linear terms are ignored, although Bonner et al. (1968) and Paegle (1969) have shown that they may contribute significantly to ageostrophic winds in the vicinity of a well-developed jet.

Solutions of equation (4) are more compact when the independent variables are nondimensional:

$$t = ft' \quad \text{and} \quad \zeta = \left(\frac{f}{K}\right)^{1/2} z. \quad (5)$$

Equation (4) has the exact solution

$$U + iV = U_g + iV_g + (W_1 + W_2 + W_3)e^{-\zeta} \quad (6)$$

where $W_1, W_2,$ and W_3 are defined by the following integrals:

$$W_1 = \frac{1}{2\sqrt{\pi\tau}} \int_0^\infty \left[e^{-\frac{(\zeta-\eta)^2}{4\tau}} - e^{-\frac{(\zeta+\eta)^2}{4\tau}} \right] x(\eta) d\eta$$

where $x(\zeta) = (U + iV)(\zeta, \tau = 0) - (U_g + iV_g)(\zeta, \tau = 0)$,

$$W_2 = \frac{\zeta}{2\sqrt{\pi}} \int_0^\tau e^{-\frac{\zeta^2}{4(\tau-\tau')}} \frac{\psi(\tau') d\tau'}{(\tau-\tau')^{3/2}}$$

where $\psi(\tau) = -(U_g + iV_g)(\zeta = 0, \tau)e^{it'}$, and (7)

$$W_3 = \frac{1}{2\sqrt{\pi}} \int_0^\tau \int_0^\infty \frac{G(\eta, \tau') \left[e^{-\frac{(\zeta-\eta)^2}{4(\tau-\tau')}} - e^{-\frac{(\zeta+\eta)^2}{4(\tau-\tau')}} \right]}{(\tau-\tau')^{1/2}} d\eta d\tau'$$

where $G(\zeta, \tau) = e^{it'} \left(\frac{\partial^2 (U_g + iV_g)}{\partial \zeta^2} - \frac{\partial (U_g + iV_g)}{\partial \tau} \right)$.

If the eddy viscosity is constant in time, then $\tau = t$. If the eddy viscosity varies with time, then τ is a more complicated function of time. We will consider an eddy viscosity with time dependence:

$$K = A(1 - \nu \cos \Omega t'), \quad 0 \leq \nu \leq 1 \quad (8)$$

in which case

$$\tau = t - \nu \frac{f}{\Omega} \sin \left(\frac{\Omega}{f} t \right),$$

and the scaling in (5) is accomplished with A replacing K . The first integral, W_1 , accounts for initial conditions, W_2 for the surface boundary condition, W_3 exists for nonzero G that occurs only if the geostrophic wind is time dependent or has curvature with height. Ching and Businger (1968) give similar integral solutions for the nonsteady boundary layer.

Integrals in equation (6) were evaluated by Gaussian quadrature for prescribed values of $K, U_g,$ and V_g . Solutions are for the initial value problem, and transient components are present together with any steady and periodic modes. With the winds initially in geostrophic balance, diurnally periodic modes dominate the solutions after several days. Results to be shown were taken from the fourth day of the integrations.

In problem 1, geostrophic components U_g and V_g are assumed to be functions of height alone. Eddy viscosity is given by equation (8) which is the same formulation as used by Ooyama (1957) except that Ooyama allowed A to vary with height. In the calculations to be shown, A is assumed to be $8 \text{ m}^2 \text{ sec}^{-1}$ implying, for the steady Eckman problem, a geostrophic wind level of 1.4 km. We set $\nu = 0.8$. The maximum K value of $14.4 \text{ m}^2 \text{ sec}^{-1}$ corresponds closely to numerical results by Krishna (1968). Minimum K is then $1.6 \text{ m}^2 \text{ sec}^{-1}$ (equation 8), and the oscillation is phased so that the minimum eddy viscosity occurs at 01 LT.

In problem 2, eddy viscosity is given a mean value of $8 \text{ m}^2 \text{ sec}^{-1}$, independent of height or time. The geostrophic wind is allowed to vary in the following way:

$$U_g + iV_g = (\tilde{U}_g + i\tilde{V}_g) - i\Delta V_0 e^{-z/H} \cos(\Omega t') \quad (9)$$

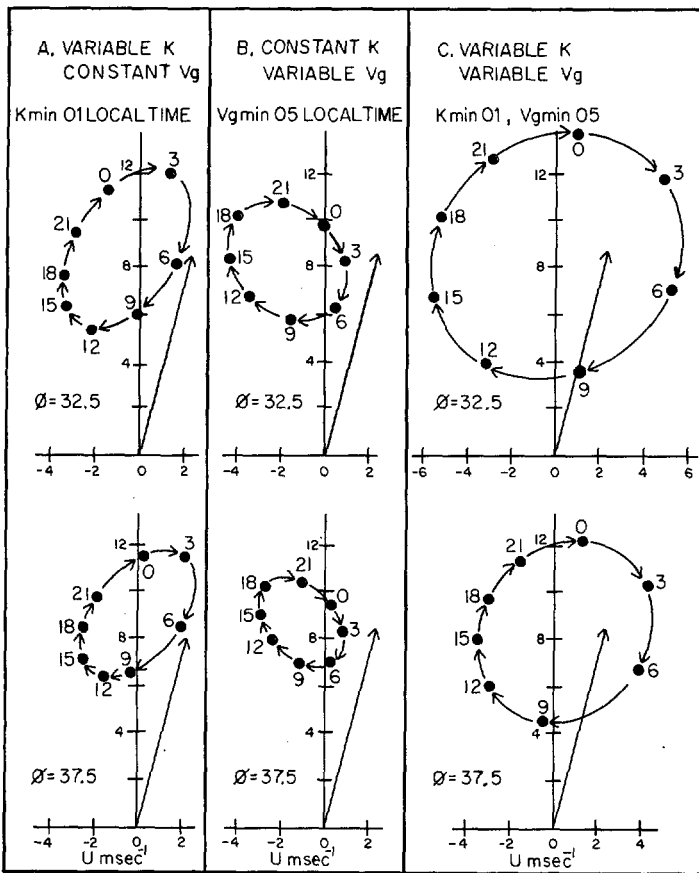


FIGURE 15.—Hodographs of wind variations from (A) variable viscosity and constant geostrophic wind, (B) constant viscosity and variable geostrophic wind, and (C) variable viscosity and variable geostrophic wind. Upper diagrams are for 32.5° latitude; lower, for 37.5° latitude. Altitude is 500 m; times are cst. Oscillations in geostrophic wind and eddy viscosity are phased to give minima at 05 and 01 cst, respectively.

where $\bar{U}_g + i\bar{V}_g$ is the time-averaged geostrophic wind at some height z above the terrain. The geostrophic variation in (9) is entirely in the y component of the wind. The variation is diurnally periodic with amplitude ΔV_0 at the surface, decreasing exponentially with height. H is set equal to 0.8 km, ΔV_0 is 3 m sec⁻¹. The oscillation is phased to give minimum and maximum V_g at 05 and 17 LT, respectively. (See preceding sections.)

In problem 3, eddy viscosity varies according to (8), geostrophic wind according to (9). We use the same values for A , ν , ΔV_0 , and H as in the previous problems.

RESULTS

Results of a series of integrations for latitudes 32.5° and 37.5° are shown in figure 15. The altitude in each case is 0.5 km, which is near the level of maximum oscillation in the model and in the observed wind.

Results from problem 1 are shown in figure 15A. At both latitudes, the oscillation from eddy viscosity variation alone is elliptical with the major axis directed slightly

to the right of the geostrophic wind. The mean amplitude of the oscillation is about 2.5 m sec⁻¹ at 37.5° and 3 m sec⁻¹ at 32.5°. Phase, orientation, and amplitude of the oscillation agree closely with results by Ooyama (1957). Maximum speed occurs between 00 and 03 LT, minimum speed near noon. The phase of the oscillation advances with latitude as would be expected from the change in the inertial period (see also Krishna 1968).

Hodographs for problem 2 (fig. 15B) show an amplitude smaller than that for problem 1. Maximum speed occurs between 18 and 21 LT—well ahead of the observed maximum in figure 14. The solution at 32.5° agrees closely with results by Holton (1967) for an isothermal atmosphere at 30° latitude.

Hodographs for problem 3 are shown in figure 15C. The amplitude of the oscillation is 4 m sec⁻¹ at 37.5° and roughly 5 m sec⁻¹ at 32.5°. Oscillations are nearly circular. Maximum wind speed occurs near midnight, minimum speed between 09 and 12 LT.

Given the very simplified treatment of the boundary layer, particularly the assumption that eddy viscosity is independent of height, we cannot expect exact agreement with results in figure 14. The amplitude of the oscillation is fairly sensitive to the mean geostrophic wind, the selection of ν , and the phase difference between eddy viscosity and pressure gradient oscillations (Paegle 1970). Solutions to problem 3, however, duplicate the major features of the observed oscillation in figure 14. Most important, comparison of results from problems 1 and 3 shows that the prescribed variation in geostrophic wind increases the amplitude of the oscillation that arises from eddy viscosity alone. *With diurnally periodic viscosity, a thermal wind oscillation giving maximum geostrophic wind in late afternoon yields a large circular oscillation in the real wind with maximum speed near midnight.*

7. SUMMARY AND CONCLUSION

Summertime geostrophic winds at terrain level in Texas and Oklahoma show day-to-night speed variations of the order of 5 to 9 m sec⁻¹. Maximum speed occurs near 17 cst, minimum speed near 05 cst. The oscillation is driven by an alternating thermal wind within the first 2 km that arises from the daily heating cycle over sloping terrain. The surface variation is explained fairly well by considering only a term $S^* \partial z / \partial x$ in the equation for V_g . However, there are significant variations in both U_g and V_g that derive from diurnal variations in the gradient of D values over the sloping terrain (Bonner and Paegle 1969).

Observed winds at Fort Worth, Tex., show a very regular diurnal oscillation with an amplitude of nearly 3 m sec⁻¹ at 600 m above the ground. This oscillation is described rather poorly by a model with constant viscosity and variable geostrophic wind, fairly well by assuming constant geostrophic wind and variable viscosity. Simulation of the real situation in this area with variable viscosity

and variable geostrophic wind yields solutions with roughly the same shape and phase as the oscillation in observed wind. The time of the geostrophic minimum is known. If we prescribe a phase lag of at least 2 hr between the geostrophic wind and eddy viscosity oscillations, the geostrophic oscillation acts to increase the amplitude that would arise from variable viscosity alone (Paegle 1970). This provides at least a partial explanation for the pronounced diurnal oscillations in boundary layer wind observed with southerly flow over the south-central United States.

ACKNOWLEDGMENTS

We wish to thank Prof. Morton Wurtele for suggesting the approach used in the theoretical portions of the study. We thank also Miss Yun-Mei Chang and Mr. Ted Tsui who did much of the computational work required in determining the geostrophic winds, and Dr. Julia Noguez de Paegle who wrote the program for determining time variations in the observed winds. Research was supported by the National Science Foundation Grant GA-698.

REFERENCES

- Bellamy, John C., "The Use of Pressure Altitude and Altimeter Corrections in Meteorology," *Journal of Meteorology*, Vol. 2, No. 1, Mar. 1945, pp. 1-79.
- Bonner, William D., "Climatology of the Low Level Jet," *Monthly Weather Review*, Vol. 96, No. 12, Dec. 1968, pp. 833-850.
- Bonner, William D., Esbensen, S., and Greenberg, R., "Kinematics of the Low-Level Jet," *Journal of Applied Meteorology*, Vol. 7, No. 3, June 1968, pp. 339-347.
- Bonner, William D., and Paegle, Jan, "Diurnal Variations in Wind and Geostrophic Wind Over the South-Central United States in Summer," *Technical Report*, Dept. of Meteorology, University of California, Los Angeles, 1969, 30 pp.
- Buajitti, Kajit, and Blackadar, A. K., "Theoretical Studies of Diurnal Wind-Structure Variations in the Planetary Boundary Layer," *Quarterly Journal of the Royal Meteorological Society*, Vol. 83, No. 358, Oct. 1957, pp. 486-500.
- Chapman, Sydney, "Atmospheric Tides and Oscillations," *Compendium of Meteorology*, 1951, pp. 510-530.
- Ching, Jason K. S., and Businger, J. A., "The Response of the Planetary Boundary Layer to Time Varying Pressure Gradient Force," *Journal of Atmospheric Sciences*, Vol. 25, No. 6, Nov. 1968, pp. 1021-1025.
- Estoque, Mariano A., "A Numerical Model of the Atmospheric Boundary Layer," *Journal of Geophysical Research*, Vol. 68, No. 4, Feb. 15, 1963, pp. 1103-1113.
- Haltiner, George J., and Martin, Frank L., *Dynamical and Physical Meteorology*, McGraw-Hill Book Co., Inc., New York, 1957, 470 pp.
- Harris, Miles F., "Diurnal and Semidiurnal Variations of Wind, Pressure, and Temperature in the Troposphere at Washington D.C.," *Journal of Geophysical Research*, Vol. 64, No. 8, Aug. 1959, pp. 983-995.
- Harris, Miles F., Finger, Frederick G., and Teweles, Sidney, "Frictional and Thermal Influences in the Solar Semidiurnal Tide," *Monthly Weather Review*, Vol. 94, No. 7, July 1966, pp. 427-447.
- Hering, Wayne S., and Borden, Thomas R., Jr., "Diurnal Variations in the Summer Wind Field Over the Central United States," *Journal of the Atmospheric Sciences*, Vol. 19, No. 1, Jan. 1962, pp. 81-86.
- Hoecker, Walter H., "Comparative Physical Behavior of Southerly Boundary-Layer Wind Jets," *Monthly Weather Review*, Vol. 93, No. 3, Mar. 1965, pp. 133-144.
- Holton, James R., "The Diurnal Boundary Layer Wind Oscillation Above Sloping Terrain," *Tellus*, Vol. 19, No. 2, 1967, pp. 199-205.
- Johnson, D. H., "Tidal Oscillations of the Lower Stratosphere," *Quarterly Journal of the Royal Meteorological Society*, Vol. 81, No. 347, Jan. 1955, pp. 1-8.
- Krishna, K., "A Numerical Study of the Diurnal Variation of Meteorological Parameters in the Planetary Boundary Layer: I. Diurnal Variation of Winds," *Monthly Weather Review*, Vol. 96, No. 5, May 1968, pp. 269-276.
- Lettau, Heinz H., "Studies of the Effects of Variations in Boundary Conditions on the Atmospheric Boundary Layer," *Annual Report 1964*, Department of Meteorology, The University of Wisconsin, Madison, 1964, pp. 99-115.
- McClain, E. Paul, "Some Effects of the Western Cordillera of North America on Cyclonic Activity," *Journal of Meteorology*, Vol. 17, No. 2, Apr. 1960, pp. 104-115.
- Ooyama, Katsuyuki, "A Study of Diurnal Variations of Wind Caused by Periodic Variation of Eddy Viscosity," *Final Report*, Contract No. AF19(604)-1368, College of Engineering, New York University, May 1957, pp. 80-135.
- Paegle, Jan, "Studies of Diurnally Periodic Boundary Layer Winds," Ph. D. thesis, Department of Meteorology, University of California, Los Angeles, 1969, 131 pp.
- Paegle, Jan, "Studies of Diurnally Periodic Boundary Layer Winds," *Technical Report*, NSF Grant GA-698, Dept. of Meteorology, University of California, Los Angeles, 1970, 69 pp.
- Sangster, Wayne E., "Diurnal Surface Geostrophic Wind Variations Over the Great Plains," *Proceedings of the Fifth Conference on Severe Local Storms*, St. Louis, Missouri, October 19-20, 1967, American Meteorological Society, Greater St. Louis Chapter, Mo., 1967, pp. 146-153.
- Sangster, Wayne E., Weather Bureau Central Region, ESSA, Kansas City, Mo., 1970 (personal communication).

[Received November 18, 1969; revised June 5, 1970]